BCB 731:

Defense Against the Dark Arts

Optimist: **A neoantigen fitness model predicts tumour response to checkpoint blockade immunotherapy**

October 30th, 2023

LETTER

doi:10.1038/nature24473

A neoantigen fitness model predicts tumour response to checkpoint blockade immunotherapy

Marta Łuksza[1], Nadeem Riaz[2,3], Vladimir Makarov[3,4], Vinod P. Balachandran[5,6,7], Matthew D. Hellmann[7,8,9], Alexander Solovyov[10,11,12,13], Naiyer A. Rizvi[14], Taha Merghoub[7,15,16], Arnold J. Levine[1], Timothy A. Chan[2,3,4,7], Jedd D. Wolchok[7,8,15,16] & Benjamin D. Greenbaum[10,11,12,13]

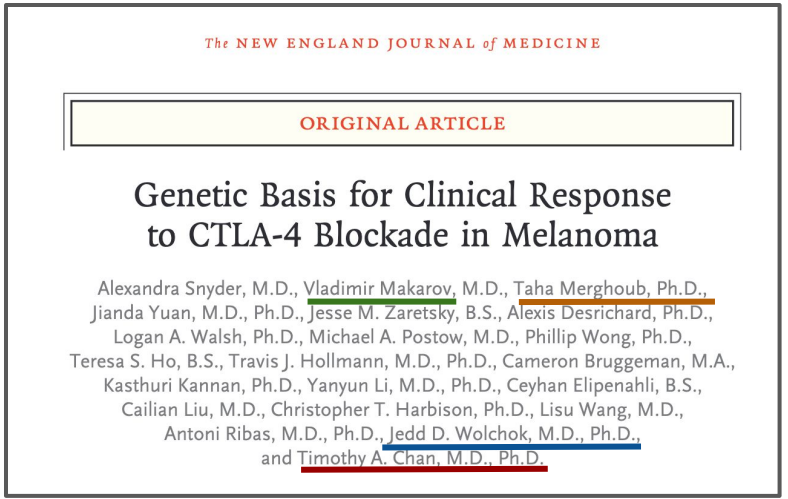

The NEW ENGLAND JOURNAL of MEDICINE

ORIGINAL ARTICLE

Genetic Basis for Clinical Response to CTLA-4 Blockade in Melanoma

Alexandra Snyder, M.D., Vladimir Makarov, M.D., Taha Merghoub, Ph.D., Jianda Yuan, M.D., Ph.D., Jesse M. Zaretsky, B.S., Alexis Desrichard, Ph.D., Logan A. Walsh, Ph.D., Michael A. Postow, M.D., Phillip Wong, Ph.D., Teresa S. Ho, B.S., Travis J. Hollmann, M.D., Ph.D., Cameron Bruggeman, M.A., Kasthuri Kannan, Ph.D., Yanyun Li, M.D., Ph.D., Ceyhan Elipenahli, B.S., Cailian Liu, M.D., Christopher T. Harbison, Ph.D., Lisu Wang, M.D., Antoni Ribas, M.D., Ph.D., Jedd D. Wolchok, M.D., Ph.D., and Timothy A. Chan, M.D., Ph.D.

Background

TMB predicts response to checkpoint blockade (Wood et al. 2020)

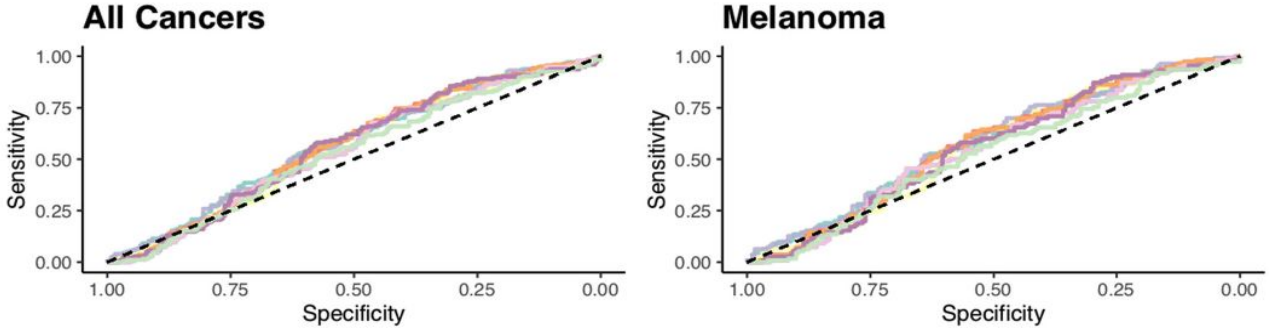

AUC by Burden and Cancer Type

Cancer type	N	TMB1	TMB2	TMB1*HLA	NB	M	A	T	M*A	M*T	A*T	M*A*T
All	431	**0.572**	0.555	0.571	0.568	0.547	0.567	0.563	0.547	0.534	0.563	0.534
Melanoma	302	0.582	0.560	**0.587**	0.572	0.550	0.572	0.558	0.550	0.529	0.558	0.529
RCC	57	0.477	0.533	0.509	0.549	**0.563**	0.556	0.552	**0.563**	0.459	0.552	0.459
NSCLC	34	0.726	0.722	0.736	**0.760**	0.740	**0.760**	0.677	0.740	0.694	0.677	0.694

Snyder et al. (2014) shows TMB predicts outlier response to aCTLA-4

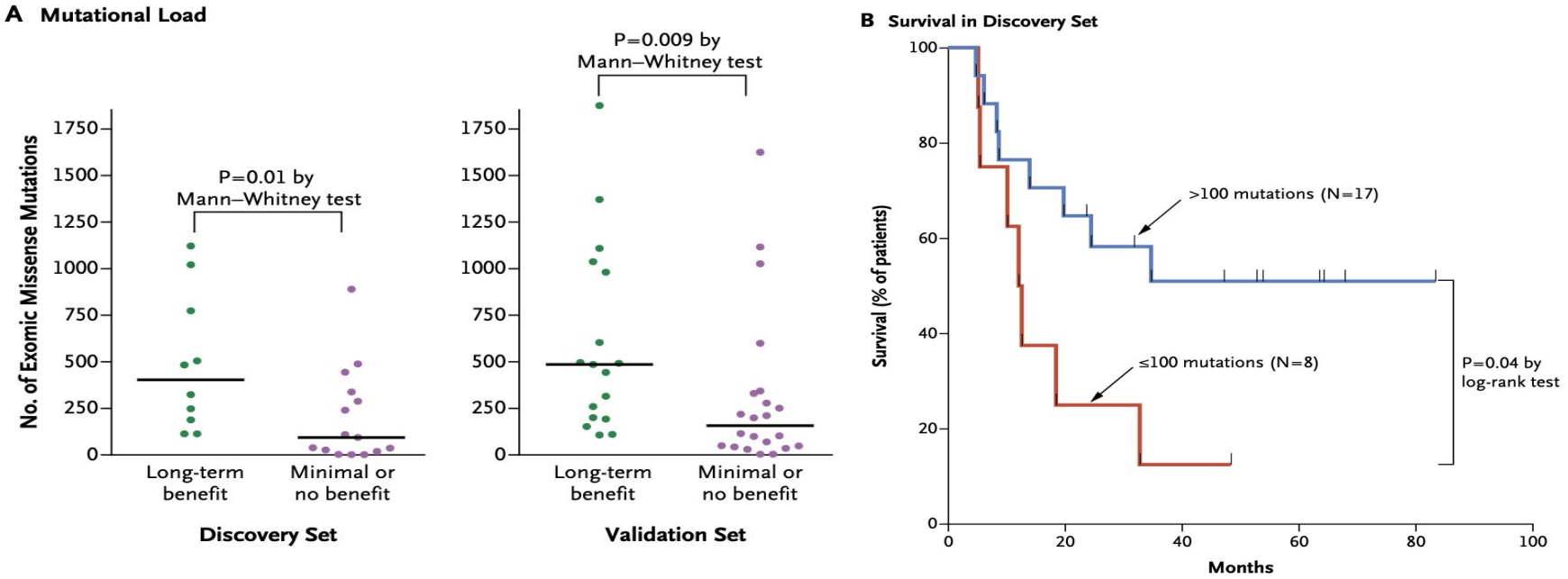

Data: Snyder et al. 2014

The NEW ENGLAND JOURNAL of MEDICINE

ORIGINAL ARTICLE

Genetic Basis for Clinical Response to CTLA-4 Blockade in Melanoma

Alexandra Snyder, M.D., Vladimir Makarov, M.D., Taha Merghoub, Ph.D., Jianda Yuan, M.D., Ph.D., Jesse M. Zaretsky, B.S., Alexis Desrichard, Ph.D., Logan A. Walsh, Ph.D., Michael A. Postow, M.D., Phillip Wong, Ph.D., Teresa S. Ho, B.S., Travis J. Hollmann, M.D., Ph.D., Cameron Bruggeman, M.A., Kasthuri Kannan, Ph.D., Yanyun Li, M.D., Ph.D., Ceyhan Elipenahli, B.S., Cailian Liu, M.D., Christopher T. Harbison, Ph.D., Lisu Wang, M.D., Antoni Ribas, M.D., Ph.D., Jedd D. Wolchok, M.D., Ph.D., and Timothy A. Chan, M.D., Ph.D.

Patient samples

All analyzed samples were collected in accordance with local Internal Review Board policies as described in ref. 8 and summarized in Table 1. Thirty-four patients had tumor samples collected prior to initiating CTLA-4 blockade, and 30 patients had samples collected after initiating CTLA-4 blockade. Clinical benefit was defined as progression-free survival lasting for greater than 24 weeks after initiation of therapy (Online Data File 1). Nine discordant lesions were present, where overall patient benefit did not match individual tumor progression. See Table 1 for details about this patient cohort.

Table 1.

Cohort summary

Group	Benefit	No benefit	Discordant
N	27	28	9
% Cutaneous	20/27	19/28	5/9
OS	3.7 (1.6–7.3)	0.8 (0.2–2.7)	4 (1.7–7.9)
Age	65 (33–81)	58.5 (18–79)	68 (40–90)
Mutations	611 (165–3,394)	321 (6–1,816)	549 (93–1,336)
Neoantigens	1,388 (209–6,502)	714.5 (3–4,510)	1,048 (197–2,584)

NOTE: Features of tumors from patients with clinical benefit, no benefit, or in which a discordant lesion was resected.

Abbreviation: OS, overall survival.

Data: Van Allen et al. (2015)

Genomic correlates of response to CTLA-4 blockade in metastatic melanoma

Eliezer M. Van Allen,[1,2,3*] Diana Miao,[1,2*] Bastian Schilling,[4,5*] Sachet A. Shukla,[1,2] Christian Blank,[6] Lisa Zimmer,[4,5] Antje Sucker,[4,5] Uwe Hillen,[4,5] Marnix H. Geukes Foppen,[6] Simone M. Goldinger,[7] Jochen Utikal,[5,8,9] Jessica C. Hassel,[10] Benjamin Weide,[11] Katharina C. Kaehler,[12] Carmen Loquai,[13] Peter Mohr,[14] Ralf Gutzmer,[15] Reinhard Dummer,[7] Stacey Gabriel,[2] Catherine J. Wu,[1,2] Dirk Schadendorf,[4,5†] Levi A. Garraway[1,2,3†]

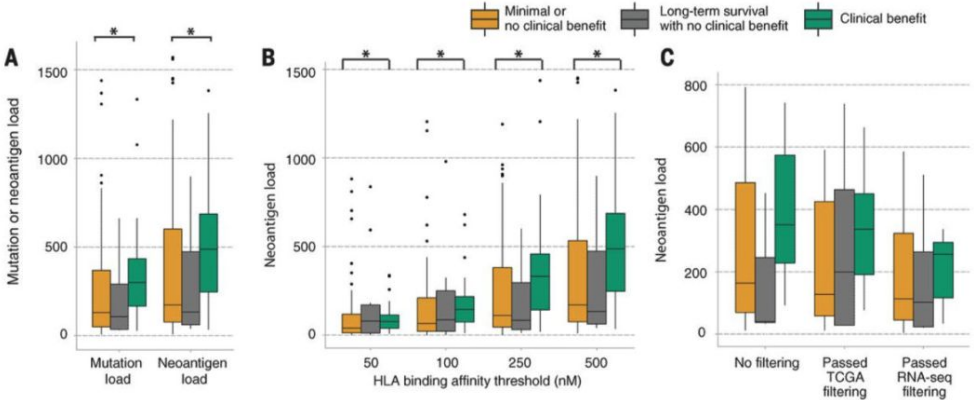

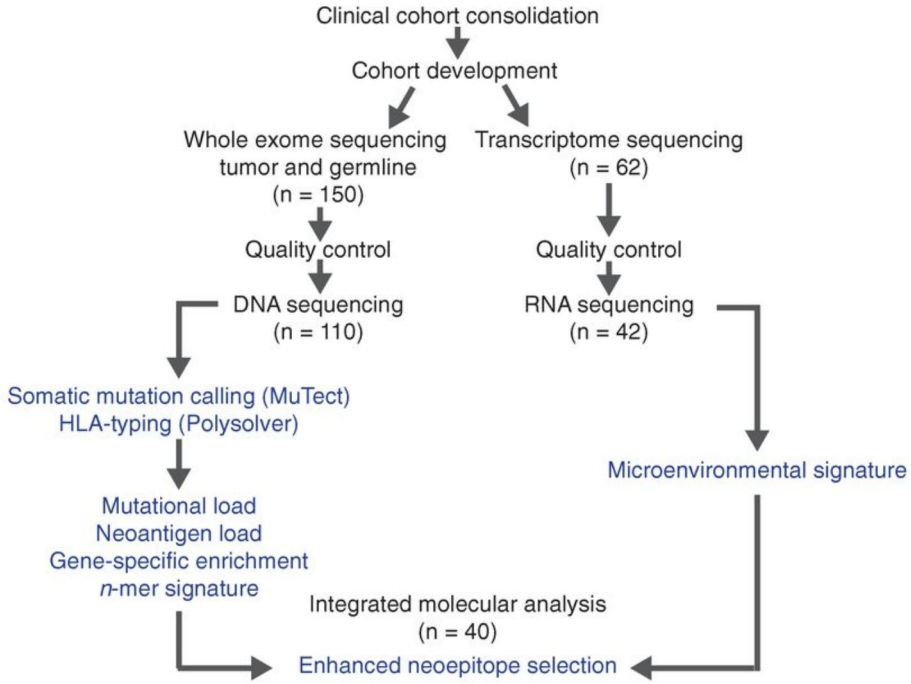

Data: Rizvi et al. (2015)

Mutational landscape determines sensitivity to PD-1 blockade in non-small cell lung cancer

Naiyer A. Rizvi,[1,2*†] Matthew D. Hellmann,[1,2*] Alexandra Snyder,[1,2,3*] Pia Kvistborg,[4] Vladimir Makarov,[3] Jonathan J. Havel,[3] William Lee,[5] Jianda Yuan,[6] Phillip Wong,[6] Teresa S. Ho,[6] Martin L. Miller,[7] Natasha Rekhtman,[8] Andre L. Moreira,[8] Fawzia Ibrahim,[1] Cameron Bruggeman,[9] Billel Gasmi,[10] Roberta Zappasodi,[10] Yuka Maeda,[10] Chris Sander,[7] Edward B. Garon,[11] Taha Merghoub,[1,10] Jedd D. Wolchok,[1,2,10] Ton N. Schumacher,[4] Timothy A. Chan[2,3,5‡]

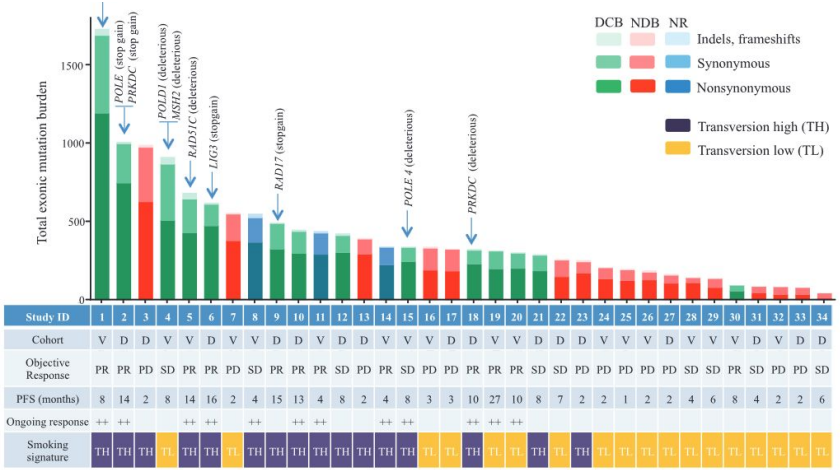

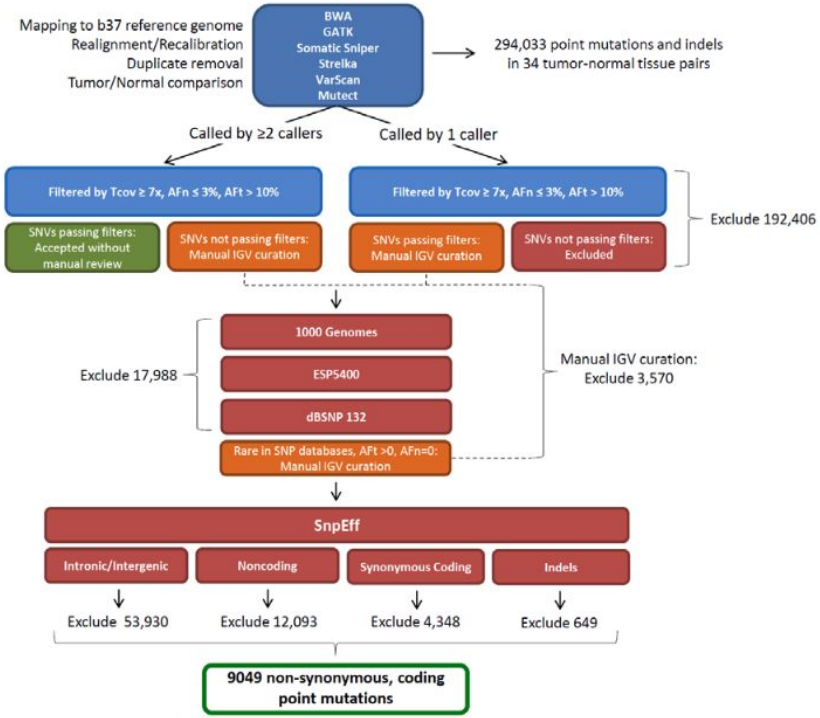

Fig. S1.
Exome analysis pipeline.

$$\frac{\hat{N}_\epsilon(t+1)}{\hat{N}(t+1)} = \frac{1}{\hat{N}(t+1)} \sum_{i:t} N_i(t) \exp[f_i - \epsilon\, C(\mathbf{a}_i, \mathbf{a}_\nu)]$$

$$H\left(\mathbf{Y}_{t+1} \middle| \hat{\mathbf{Y}}_{t+1}\right) = \sum_{\nu \in K(t)} Y_\nu(t+1)\, \log\left[Y_\nu(t+1) / \hat{Y}_\nu(t+1)\right]$$

$$\frac{p}{p_0} \sim \exp\left[\sum_t \Delta\mathcal{H}(t)\right] \qquad \Delta\mathcal{H}(t) = \tilde{m}(t)\left[-H\left(\mathbf{Y}_{t+1} \middle| \hat{\mathbf{Y}}_{t+1}\right) + H(\mathbf{Y}_{t+1} | \mathbf{Y}_t)\right]$$

Physicists predict pathogen fitness

ARTICLE

doi:10.1038/nature13087

A predictive fitness model for influenza

Marta Łuksza[1,2] & Michael Lässig[1]

The seasonal human influenza A/H3N2 virus undergoes rapid evolution, which produces significant year-to-year sequence turnover in the population of circulating strains. Adaptive mutations respond to human immune challenge and occur primarily in antigenic epitopes, the antibody-binding domains of the viral surface protein haemagglutinin. Here we develop a fitness model for haemagglutinin that predicts the evolution of the viral population from one year to the next. Two factors are shown to determine the fitness of a strain: adaptive epitope changes and deleterious mutations outside the epitopes. We infer both fitness components for the strains circulating in a given year, using population-genetic data of all previous strains. From fitness and frequency of each strain, we predict the frequency of its descendent strains in the following year. This fitness model maps the adaptive history of influenza A and suggests a principled method for vaccine selection. Our results call for a more comprehensive epidemiology of influenza and other fast-evolving pathogens that integrates antigenic phenotypes with other viral functions coupled by genetic linkage.

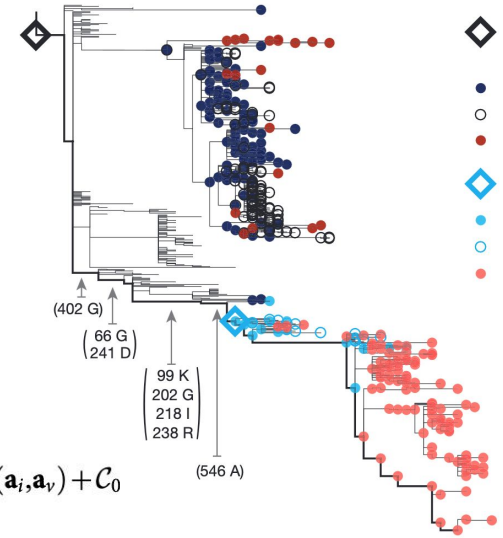

$$x_i = \frac{1}{z_\epsilon(t)}\left[\frac{m_i}{m(t)} + \frac{\epsilon}{m_{\nu(i,\kappa)}(t)}\right]$$

$$\hat{Y}_\nu(t+1) = \sum_{i \in S(t)} \breve{\rho}_{i,\nu} x_i \exp(f_i) \quad \text{for } \nu \in K(t)$$

$$\Delta\mathcal{H}_{\text{tot}} = \sum_t \Delta\mathcal{H}\left(t; \sigma^*_{\text{ep}}(t), D^*_0, \sigma^*_{\text{ne}}, \lambda^*(t)\right)$$

$$\hat{X}_\nu(t+1, \epsilon) = \sum_{i:\nu,t} x_i \exp[f_i(\epsilon = 0) - \epsilon\, C(\mathbf{a}_i, \mathbf{a}_\nu) + \mathcal{C}_0$$

$$\hat{\mathcal{C}}_\nu(t+1) = \sum_{i:t} x_i \exp(f_i) \mathcal{C}(\mathbf{a}_i,$$

$$\bar{\Phi}\left(\tilde{\mathbf{Y}}, t+1\right) = \sum_{\nu \in K(t)} \Phi_\nu(t) \tilde{Y}_\nu$$

$$\left(\sigma^*_{\text{ep}}(t), \lambda^*(t)\right) = \arg\max_{\sigma_{\text{ep}}, \lambda} \sum_{t'=t-8} \Delta\mathcal{H}\left(t'; \sigma_{\text{ep}}, D^*_0, \sigma^*_{\text{ne}}, \lambda\right)$$

$$f_i^{\text{lin}} = \sigma_{\text{ep}} D_{\text{ep}}\left(\mathbf{a}_i, \mathbf{a}^*(t)\right) - \sigma_{\text{ne}} D_{\text{ne}}\left(\mathbf{a}_i, \mathbf{a}_i^*\right)$$

$$\text{Var}\ \Phi(t) = \sum_{\nu \in K(t)} Y_\nu(t)\left[\Phi_\nu(t) - \bar{\Phi}(t)\right]^2 = \text{Var}\ F(t)$$

$$F_\nu(t) = \log \frac{\hat{Y}_\nu(t+1)}{Y_\nu(t)} \qquad \breve{S}^{(\kappa)}_\nu(t) = \breve{S}^{(\kappa)}_\nu \cap S(t) \quad \text{for } \nu \in K(t)$$

$$\breve{\rho}_{i,\nu} = \frac{1}{n} \sum_{\kappa=1}^{n} \breve{\epsilon}^{(\kappa)}_{i,\nu} \quad \text{with } \breve{\epsilon}^{(\kappa)}_{i,\nu} = \begin{cases} 1 & \text{if } i \in \breve{S}^{(\kappa)}_\nu \\ 0 & \text{otherwise} \end{cases}$$

$$\bar{\Phi}(t+1) = \sum_{\nu \in K(t)} \Phi_\nu(t) Y_\nu(t+1)$$

$$V = \frac{1}{\Delta t} \sum_t \sum_{\nu \in K(t)} Y_\nu(t)[F_\nu(t) - \bar{F}(t)]^2$$

$$\Delta\mathcal{H}(t) = \tilde{m}(t) \sum_{\nu \in K(t)} Y_\nu(t+1) F_\nu(t)$$

$$f_i(\epsilon) = f_i(\epsilon = 0) - \epsilon\, \mathcal{C}(\mathbf{a}_i, \mathbf{a}_\nu) + \mathcal{C}_0(\epsilon)$$

$$\mathcal{Y}(\Phi, t) = \int d\Phi\, Y_\nu(t)\, \delta(\Phi - \Phi_\nu(t))$$

Łuksza pathogen fitness model

Our prediction is based on frequency and fitness data that depend only on information actually available at a given point in time. Consider a clade v containing a set of strains i with frequencies x_i in a given season t. The observed frequency of that clade in season t, which is denoted as $X_v(t)$, is simply the sum of these strain frequencies, $X_v(t) = \sum_{i:v,t} x_i$. This sum is defined as an average over strain trees, as detailed in Methods. Each strain has a Malthusian fitness or growth rate f_i (measured in units of 1/year), which is to be specified by our model. Given these initial data, we predict the frequency of that clade in the season 1 year later,

$$\hat{X}_v(t+1) = \sum_{i:v,t} x_i \exp(f_i) \tag{1}$$

Non-epitope mutations are predominantly under negative selection[9], because they affect protein stability and other conserved molecular functions[13,14]. Here we describe these effects by a simple mutational-load model: each strain incurs a fitness cost $\mathcal{L}(\mathbf{a}_i)$ that is the cumulative effect of recent non-epitope amino acid changes, which occur in its ancestral lineage in the current season (Methods).

Together we obtain a strain fitness of the form

$$f_i = f_0 - \mathcal{L}(\mathbf{a}_i) - \sum_{j:\, t_j < t_i} x_j \mathcal{C}(\mathbf{a}_i, \mathbf{a}_j) \tag{2}$$

with a constant f_0 ensuring the correct normalization of strain frequencies (Methods). Importantly, this strain-based model goes beyond a fitness model for individual mutations: it counts each new beneficial or

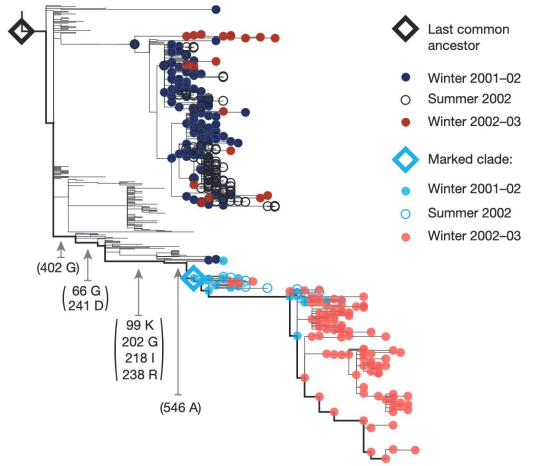

Prediction of cross-immunity. Another aggregate variable suitable for predictions is the average cross-immunity between a given strain v and the circulating strains in a given season,

$$\mathcal{C}_v(t) \equiv \sum_{i:t} x_i \mathcal{C}(\mathbf{a}_i, \mathbf{a}_v) \tag{24}$$

Our model predicts the expected average cross-immunity in season $t + 1$,

$$\hat{\mathcal{C}}_v(t+1) = \sum_{i:t} x_i \exp(f_i) \mathcal{C}(\mathbf{a}_i, \mathbf{a}_v) \tag{25}$$

Tumor clonal structure

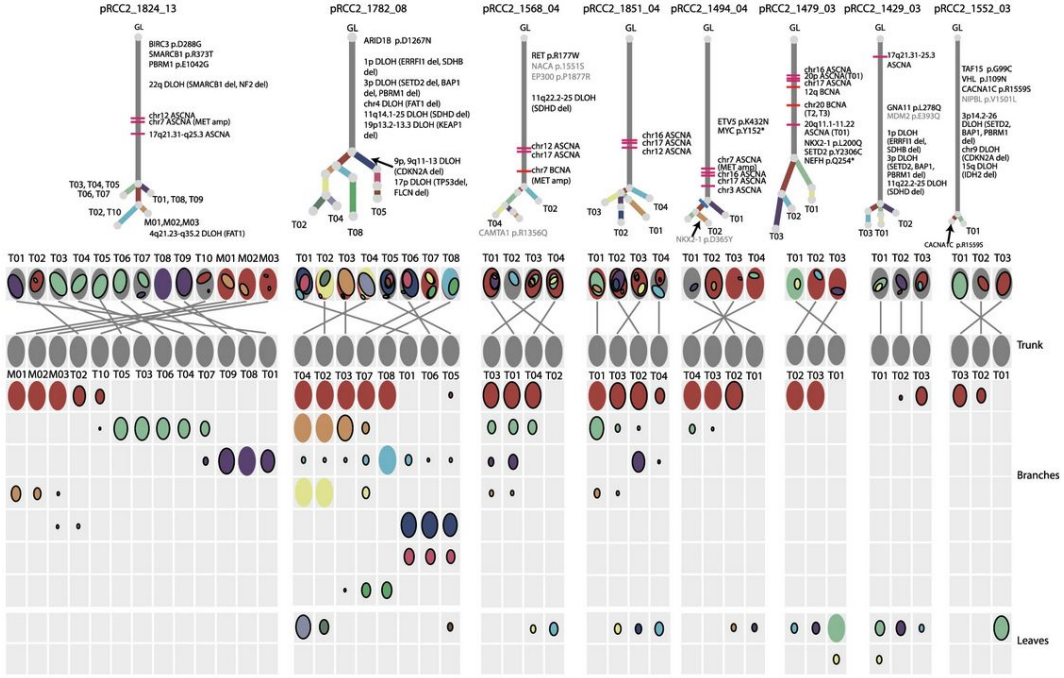

https://doi.org/10.1038/s41467-020-16546-5 OPEN

The genomic and epigenomic evolutionary history of papillary renal cell carcinomas

“Drivers”, clonality, allele frequency

Modeling the subclonal evolution of cancer cell populations

Diego Chowell[1,2,‡], **James Napier**[3], **Rohan Gupta**[3], **Karen S. Anderson**[2,4], **Carlo C. Maley**[2,4,5,6,*], and **Melissa A. Wilson Sayres**[2,4,7,*]

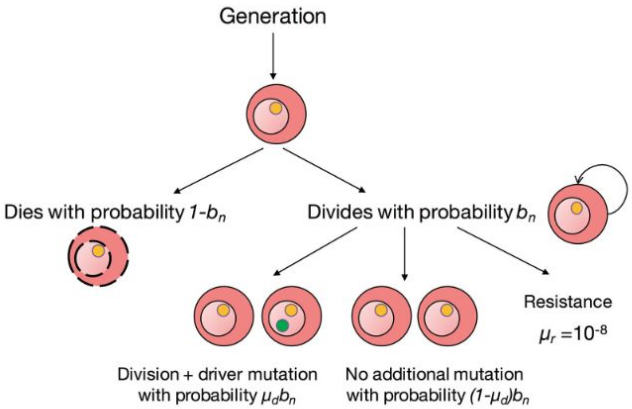

Figure 1.
Branching evolutionary process of cancer. Schematic representation of the process developed to simulate the subclonal evolution of cancer is presented below. For details of the process and assumptions, see main Quick Guide to Equations and Assumptions.

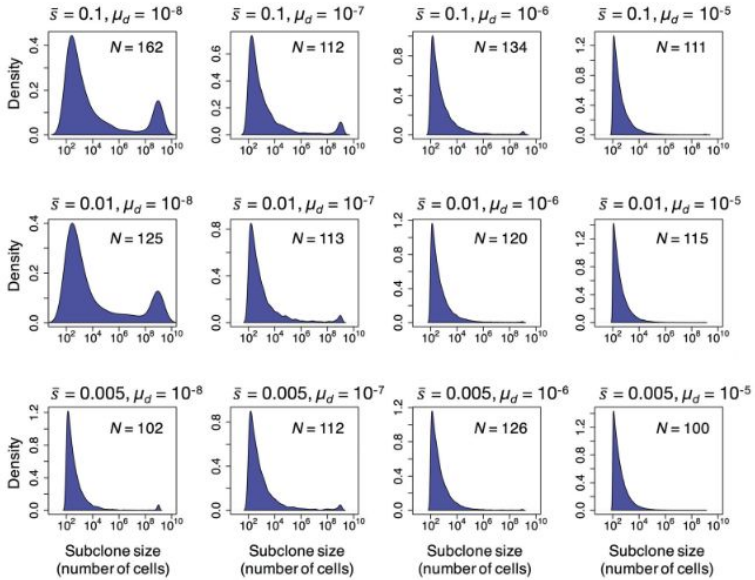

PhyloWGS: reconstructing cancer phylogenies from sequencing data

Deshwar *et al. Genome Biology* (2015) 16:35
DOI 10.1186/s13059-015-0602-8

METHOD Open Access

PhyloWGS: Reconstructing subclonal composition and evolution from whole-genome sequencing of tumors

Amit G Deshwar[1], Shankar Vembu[2], Christina K Yung[3], Gun Ho Jang[3], Lincoln Stein[3,5] and Quaid Morris[1,2,4,5*]

Abstract

Tumors often contain multiple subpopulations of cancerous cells defined by distinct somatic mutations. We describe a new method, PhyloWGS, which can be applied to whole-genome sequencing data from one or more tumor samples to reconstruct complete genotypes of these subpopulations based on variant allele frequencies (VAFs) of point mutations and population frequencies of structural variations. We introduce a principled phylogenic correction for VAFs in loci affected by copy number alterations and we show that this correction greatly improves subclonal reconstruction compared to existing methods. PhyloWGS is free, open-source software, available at https://github.com/morrislab/phylowgs.

PhyloWGS: identifying sub-clones by allele fraction clustering

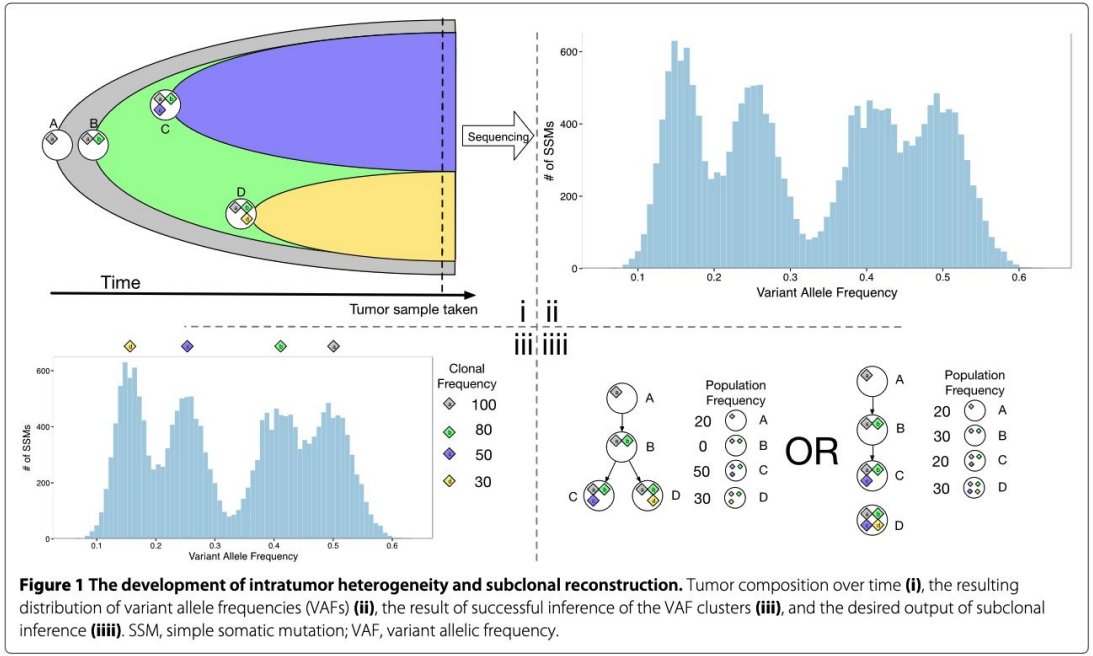

Figure 1 The development of intratumor heterogeneity and subclonal reconstruction. Tumor composition over time **(i)**, the resulting distribution of variant allele frequencies (VAFs) **(ii)**, the result of successful inference of the VAF clusters **(iii)**, and the desired output of subclonal inference **(iiii)**. SSM, simple somatic mutation; VAF, variant allelic frequency.

PhyloWGS: adjusting for tumor "purity" / normal "contamination"

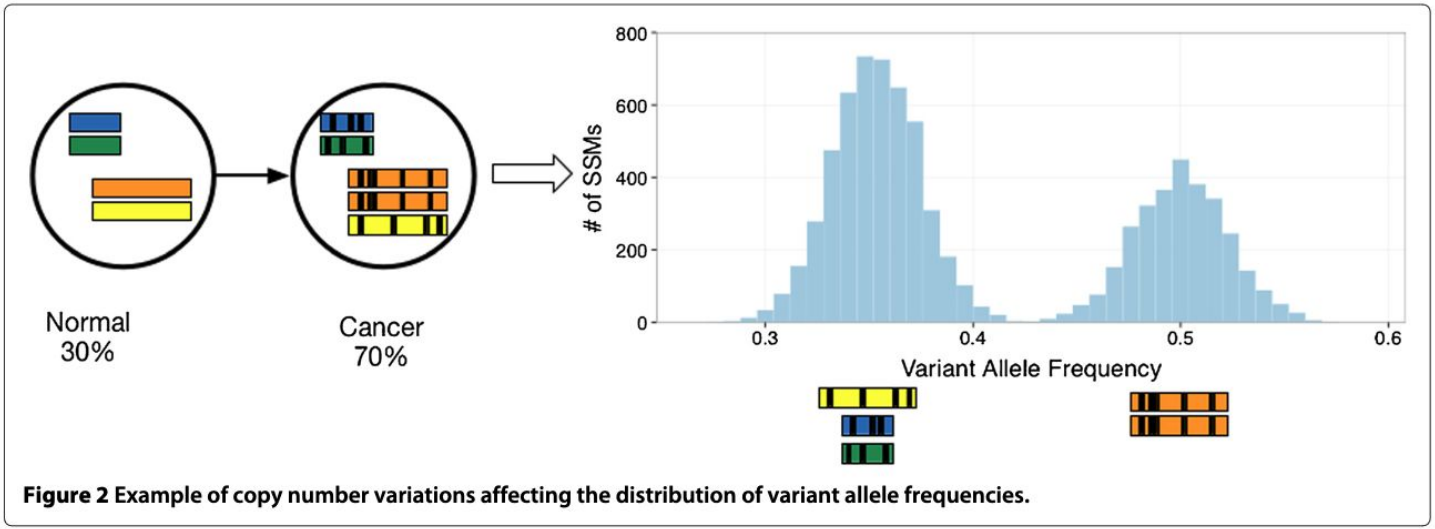

Figure 2 Example of copy number variations affecting the distribution of variant allele frequencies.

PhyloWGS: adjusting for copy number changes

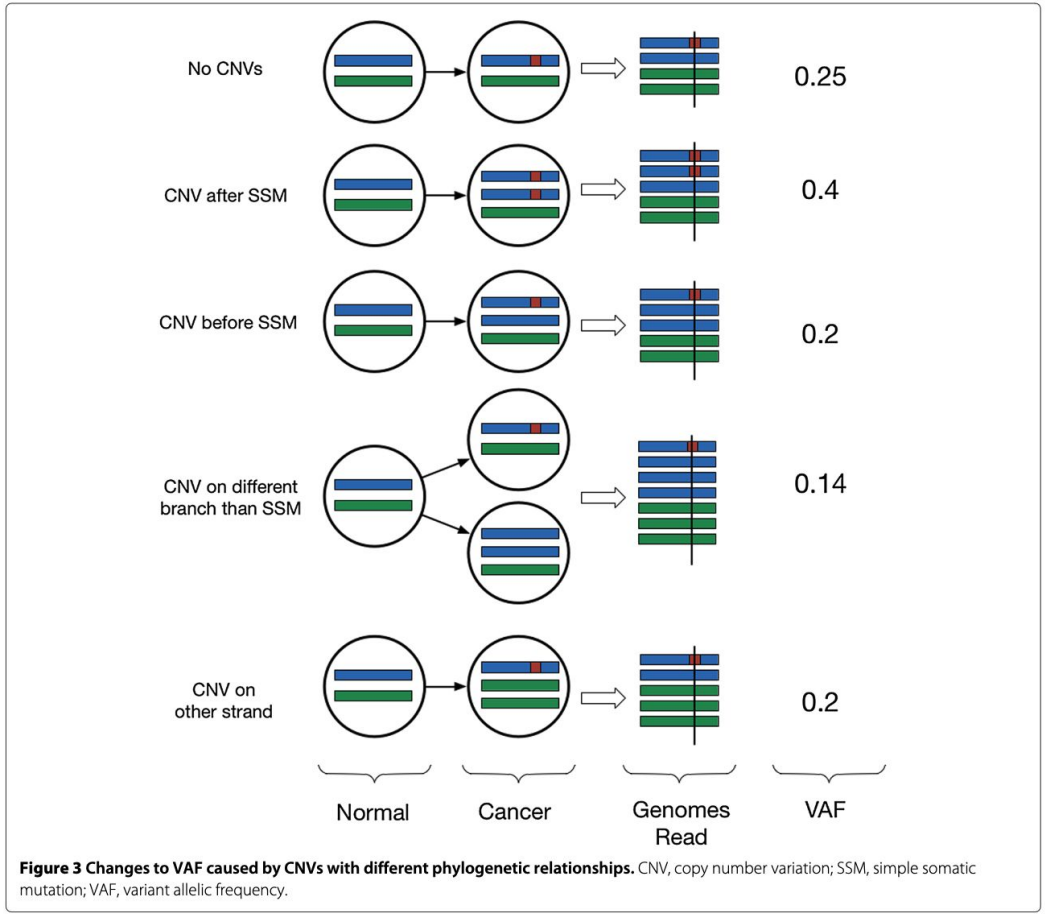

Figure 3 Changes to VAF caused by CNVs with different phylogenetic relationships. CNV, copy number variation; SSM, simple somatic mutation; VAF, variant allelic frequency.

The Paper

Let's apply the pathogen fitness model to tumor phylogenies

A neoantigen fitness model predicts tumour response to checkpoint blockade immunotherapy

Marta Łuksza[1], Nadeem Riaz[2,3], Vladimir Makarov[3,4], Vinod P. Balachandran[5,6,7], Matthew D. Hellmann[7,8,9], Alexander Solovyov[10,11,12,13], Naiyer A. Rizvi[14], Taha Merghoub[7,15,16], Arnold J. Levine[1], Timothy A. Chan[2,3,4,7], Jedd D. Wolchok[7,8,15,16] & Benjamin D. Greenbaum[10,11,12,13]

$$n(\tau) = \sum_{\alpha} X_{\alpha} \exp(F_{\alpha}\tau)$$

We propose a fitness model of tumour–immune interactions as a general mathematical framework to describe the evolutionary dynamics of cancer cell populations under checkpoint blockade immunotherapy and provide a proof of concept for its utility (Fig. 1). Analogous fitness models based on immune interactions have been successfully applied to human influenza[7], HIV[8] and chronic viral infections[9]. Checkpoint blockade exposes cancer cells to strong immune pressure on their neoantigens, reducing their reproductive success. Our model predicts the evolutionary dynamics of a cancer cell population after a finite time under such pressure. We compute $n(\tau)$, the predicted future effective size of a cancer cell population in a tumour relative to its effective size at the start of therapy. The size is a weighted sum over all of the genetic clones of a tumour (Fig. 1a and Methods),

$$n(\tau) = \sum_{\alpha} X_{\alpha} \exp(F_{\alpha}\tau) \quad (1)$$

Basic idea

- Use PhyloWGS to infer clones and their evolutionary relationship from tumor + normal DNA sequencing
- Define immune fitness of each sub-clone in terms of predicted neoantigens

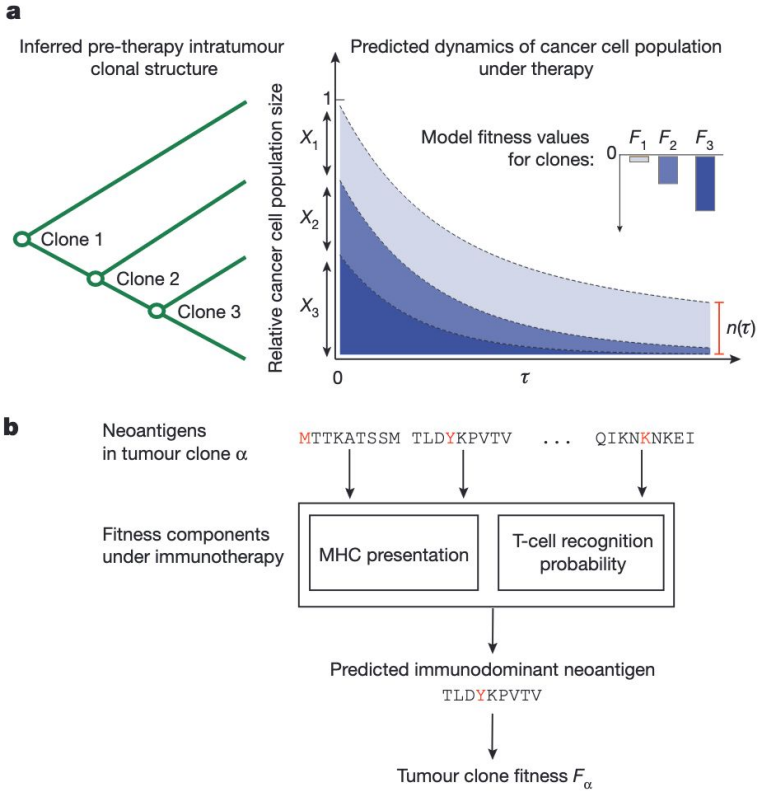

Fitness ~= immunogenicity of dominant neoantigen in the clone

(Fig. 1b and Methods). Here we model the fitness of a given clone α by the recognition potential of its dominant neoantigen,

$$F_\alpha = -\max_{i \in \text{clone } \alpha} (A_i \times R_i) \quad (2)$$

Recognition potential: “R” and “A”

$$n(\tau) = \sum_{\alpha} X_{\alpha} \exp\left(- \max_{i \in \text{ clone } \alpha} (A_i \times R_i)\, \tau \right) \tag{5}$$

$$A = K_{\mathrm{d}}^{\mathrm{WT}} / K_{\mathrm{d}}^{\mathrm{MT}} \tag{7}$$

$$R = Z(k)^{-1} \sum_{e \in \mathrm{IEDB}} \exp(-k(a - |\boldsymbol{s}, \boldsymbol{e}|)) \tag{10}$$

Predicted tumor sizes

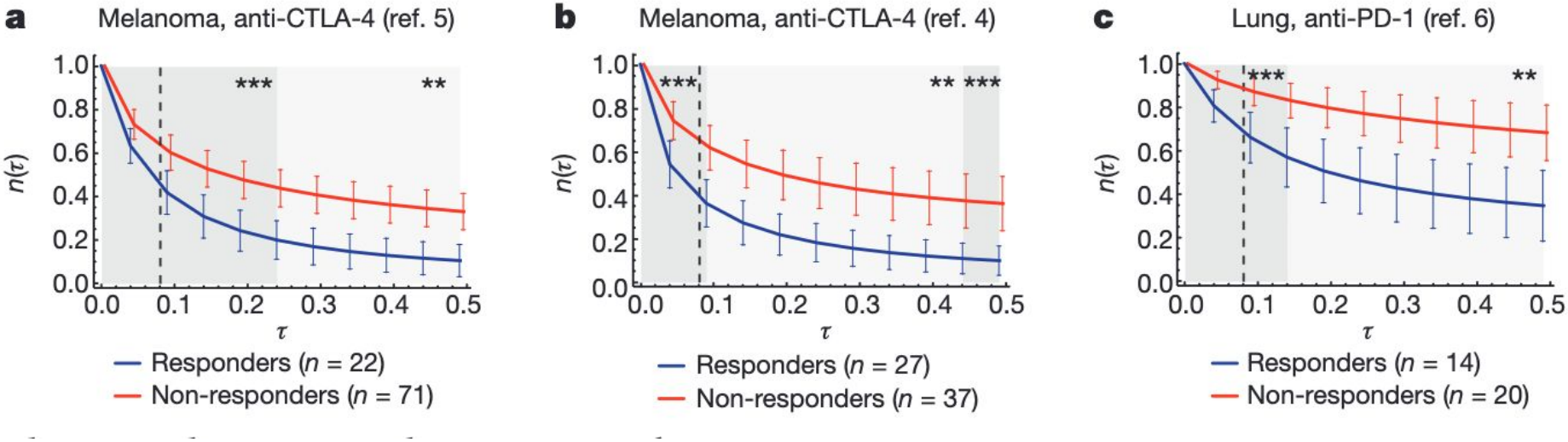

Survival stratified by fitness

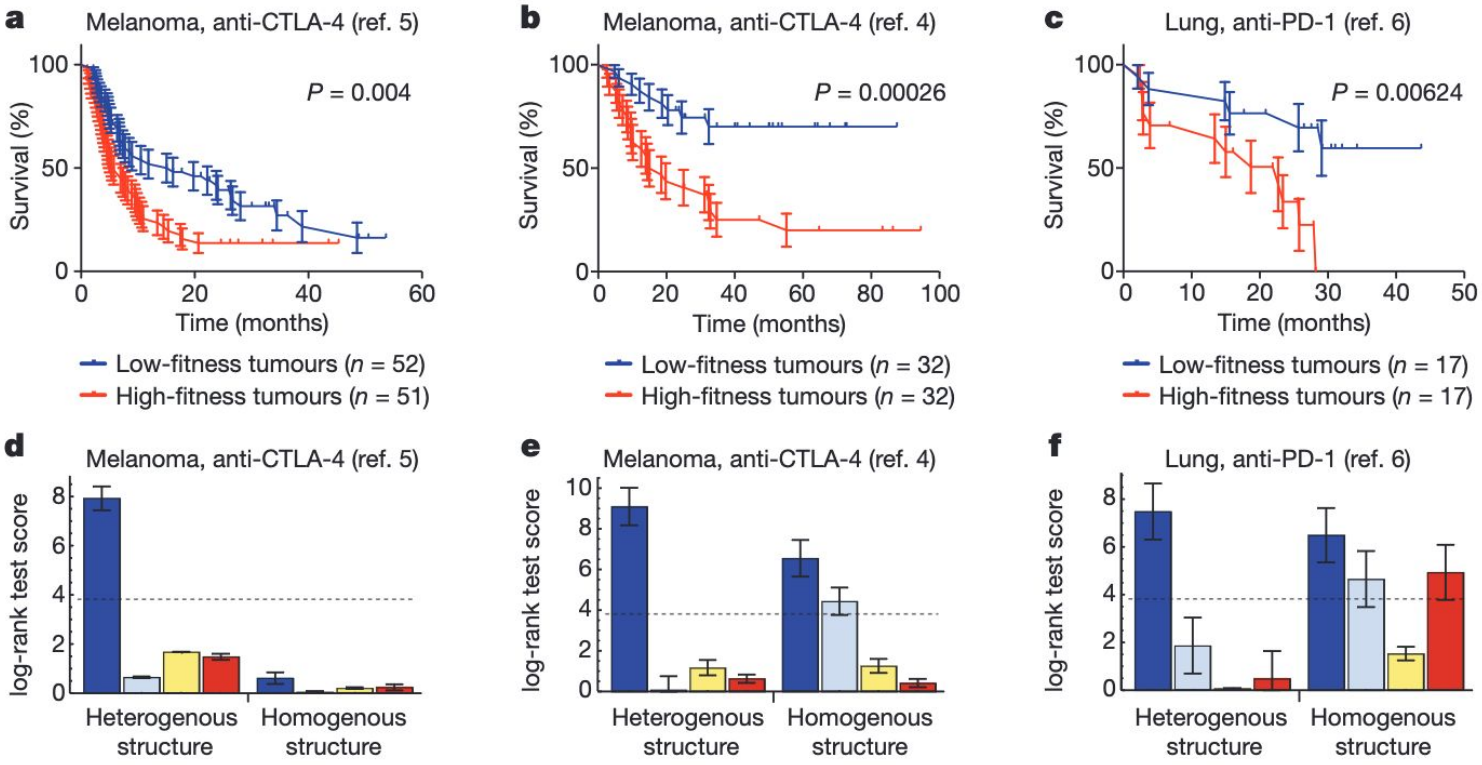

Homework

Data

Sample	Months	Status
Pat02	53.6547357	0
Pat03	3.28766763	1
Pat04	32.4492795	0
Pat06	5.29314488	1
Pat08	4.60273468	1
Pat100	11.8356035	1
Pat101	9.46848277	1
Pat103	34.4547568	1
Pat104	7.79177228	1
Pat106	8.21916908	1
Pat109	2.72876413	1
Pat11	25.9725743	0
Pat110	10.5205364	1
Pat113	9.89587957	1
Pat115	4.76711806	1
Pat117	30.0492821	0
Pat118	10.2903997	1
Pat119	26.5643545	0
Pat121	4.01095451	1
Pat123	28.0438049	1
Pat124	4.79999474	1
Pat126	21.0739495	0
Pat127	10.9150565	1
Pat128	3.71506442	1
Pat129	17.7205285	0
Pat13	24.0657271	1
Pat130	1.47945043	1
Pat131	8.44930581	1
Pat132	22.2246332	0
Pat133	17.8191586	1
Pat135	2.66301078	1
Pat138	48.5917276	1
Pat139	3.25479095	1

Survival VanAllen et al. | Survival Snyder et al. | Survival Rizvi et al.

ID	MUTATION_	Sample	WT.Peptide	MT.Peptide	MT.Allele	WT.Score	MT.Score	HLA
1	1_44084332_	AL4602	RGTETCGLI	RVTETCGLI	C1502	1208	124	A0301,A3201,B0801,B5101,C0702,C1502
2	1_56990069_	AL4602	IGRLRPHFL	IVRLRPHFL	B0801	305	165	A0301,A3201,B0801,B5101,C0702,C1502
3	1_15219203	AL4602	SSNGPHGSV	SSNVPHGSV	C1502	73	210	A0301,A3201,B0801,B5101,C0702,C1502
4	1_15822729	AL4602	ALWFRKRCF	ALWFRKLCF	A3201	547	284	A0301,A3201,B0801,B5101,C0702,C1502
5	1_15941037	AL4602	NTREHDQLI	NSREHDQLI	C1502	41	42	A0301,A3201,B0801,B5101,C0702,C1502
6	1_15950577	AL4602	MKRKNFTEV	MKRKNFTEL	B0801	258	63	A0301,A3201,B0801,B5101,C0702,C1502
7	1_23134964	AL4602	HTLTFFING	HTLTFFINW	A3201	11745	59	A0301,A3201,B0801,B5101,C0702,C1502
8	1_24836727	AL4602	RAFMKILGK	RALMKILGK	A0301	36	89	A0301,A3201,B0801,B5101,C0702,C1502
9	1_24836727	AL4602	EVTRAFMKI	EVTRALMKI	C1502	241	327	A0301,A3201,B0801,B5101,C0702,C1502
10	10_7357937	AL4602	LTVHVTQPK	LTVHMTQPK	A0301	442	460	A0301,A3201,B0801,B5101,C0702,C1502
11	11_2064826	AL4602	KVVYFTATF	KVVYFMATF	A3201	5	11	A0301,A3201,B0801,B5101,C0702,C1502
12	11_2064826	AL4602	VYFTATFPY	VYFMATFPY	C0702	162	220	A0301,A3201,B0801,B5101,C0702,C1502
13	11_2064826	AL4602	TSGKVVYFT	TSGKVVYFM	C1502	8765	430	A0301,A3201,B0801,B5101,C0702,C1502
14	11_5532201	AL4602	NVQEIVFVV	NVHEIVFVV	C1502	341	222	A0301,A3201,B0801,B5101,C0702,C1502
15	11_5611444	AL4602	ALKRTLTNR	ALKRTFTNR	A0301	670	359	A0301,A3201,B0801,B5101,C0702,C1502
16	11_5611444	AL4602	RTLTNRFKI	RTFTNRFKI	A3201	36	14	A0301,A3201,B0801,B5101,C0702,C1502
17	11_5611444	AL4602	LTNRFKIPI	FTNRFKIPI	A3201	104	377	A0301,A3201,B0801,B5101,C0702,C1502
18	11_5611444	AL4602	RTLTNRFKI	RTFTNRFKI	C1502	136	154	A0301,A3201,B0801,B5101,C0702,C1502
19	11_5611444	AL4602	LTNRFKIPI	FTNRFKIPI	C1502	148	78	A0301,A3201,B0801,B5101,C0702,C1502
20	11_6313776	AL4602	ISIPLDSNM	ISIQLDSNM	C1502	310	452	A0301,A3201,B0801,B5101,C0702,C1502
21	11_8287819	AL4602	QVDEHSKPP	QVDEHSKPL	C1502	17298	178	A0301,A3201,B0801,B5101,C0702,C1502
22	12_4662254	AL4602	VKVKSPVEK	VMVKSPVEK	A0301	19358	89	A0301,A3201,B0801,B5101,C0702,C1502
23	12_4662254	AL4602	KVKSPVEKK	MVKSPVEKK	A0301	99	155	A0301,A3201,B0801,B5101,C0702,C1502
24	12_9334662	AL4602	IARMFIFAI	NARMFIFAI	B0801	667	145	A0301,A3201,B0801,B5101,C0702,C1502
25	12_2100797	AL4602	ALSFSYIAK	VLSFSYIAK	A0301	27	24	A0301,A3201,B0801,B5101,C0702,C1502
26	12_2100797	AL4602	KMFLAALSF	KMFLAVLSF	A3201	4	3	A0301,A3201,B0801,B5101,C0702,C1502
27	12_2100797	AL4602	LAALSFSYI	LAVLSFSYI	B5101	295	282	A0301,A3201,B0801,B5101,C0702,C1502
28	12_2105140	AL4602	AMGFQSMV	ATGFQSMVI	A3201	75	125	A0301,A3201,B0801,B5101,C0702,C1502
29	12_2105140	AL4602	LAMGFQSM	LATGFQSMV	C1502	49	181	A0301,A3201,B0801,B5101,C0702,C1502
30	12_2105140	AL4602	AMGFQSMV	ATGFQSMVI	C1502	2826	79	A0301,A3201,B0801,B5101,C0702,C1502
31	12_2539828	AL4602	VVGAGGVGI	VVGASGVGK	A0301	410	217	A0301,A3201,B0801,B5101,C0702,C1502
32	12_5282062	AL4602	LSGEGVSPV	LSGEVVSPV	C1502	771	238	A0301,A3201,B0801,B5101,C0702,C1502
33	12_5282062	AL4602	GVSPVNISV	VVSPVNISV	C1502	2091	364	A0301,A3201,B0801,B5101,C0702,C1502

VanAllen et al. | Snyder et al. | Rizvi et al.


Fin